

# Asymmetric Cylindrical Gears

Dr. Paul Langlois and Baydu Al

## Introduction

In typical applications the two flanks of a given cylindrical gear have different operating conditions with, for example, different loads and different periods of operation. This is the case for automotive gear trains where the operation is mostly unidirectional with the primary drive flanks operating for a much greater time and under greater load than the coast flanks. Asymmetric cylindrical gears using a different pressure angle on each flank can be designed to improve the performance on the drive flank at the expense of the coast. Asymmetric gears have been used for many years — especially in high-cost, low-volume applications such as wind and aerospace. Significant application and interest for asymmetric gears is now being shown within the automotive industry. With this increasing interest comes an increasing need for methods and tools to assess the relative merits of asymmetric gears, as compared to symmetric gears, and assess the impact of changes in asymmetric gear geometry. The standard rating methods for symmetric cylindrical gears are not directly applicable to asymmetric gears. In this paper we present a loaded tooth contact analysis (LTCA) method for asymmetric gears that provides an accurate and efficient design tool for analyzing and comparing designs. The presented method is implemented in SMT’s MASTA software. We further present an example comparative study using this tool for an example automotive application.

## Asymmetric Gear Geometry and Rating

**Drive-side geometry.** Asymmetric cylindrical gears are involute cylindrical gears with asymmetric flank profiles. In particular, the usual approach is to increase the operating pressure angle on the drive flank beyond the traditional limits of symmetric gears by using a lower pressure angle on the coast flank to maintain sufficient tip thickness. Such a design can lead to benefits that include an increased transverse contact ratio on the drive-side, leading to lower sliding and, therefore, less scuffing risk and higher efficiency. The increased pressure angle on the drive flank results in a smaller base radius, which gives a higher normal load for a given torque. However, it also leads to a larger radius of curvature at contact, potentially leading to lower contact stresses. Decreased bending stresses can also result due to a decreased bending moment on the gear tooth. Higher strength on the drive-side can lead to more compact, lower weight designs.

**Coast-side geometry.** With an increased pressure angle on the drive-side, a decreased pressure angle on the coast-side is required to maintain tip thickness. This decreased pressure angle often leads to NVH benefits for the drive-side with the increased tooth compliance. One of the biggest challenges when designing asymmetric gears for applications where operation on both flanks does occur is to limit the decrease in performance on the coast-side. In an automotive application, for example, particular attention should be paid to NVH performance in coasting conditions.

It is worth noting that for idler gears, operating on both flanks in the same operating conditions, there may be additional benefits with asymmetric gears. In a planetary system the planet gears operate on both flanks. Typically, the sun to planet mesh fails before the planet to annulus. Using a higher pressure angle on the sun-side and lower on the annulus, the lives between the meshes can be balanced.

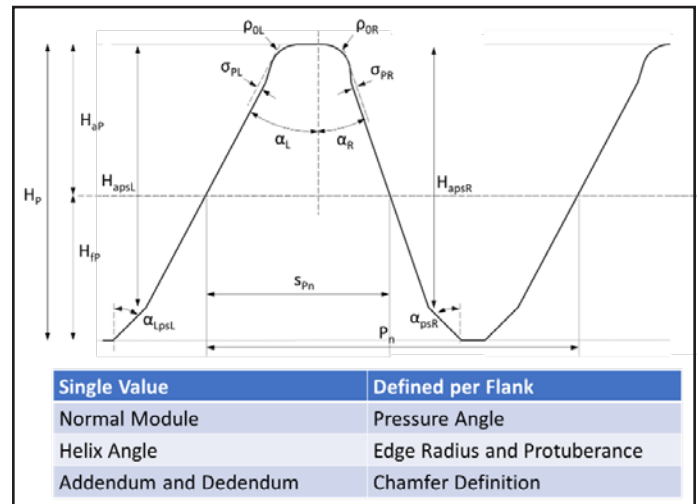


Figure 1 Asymmetric rack geometry.

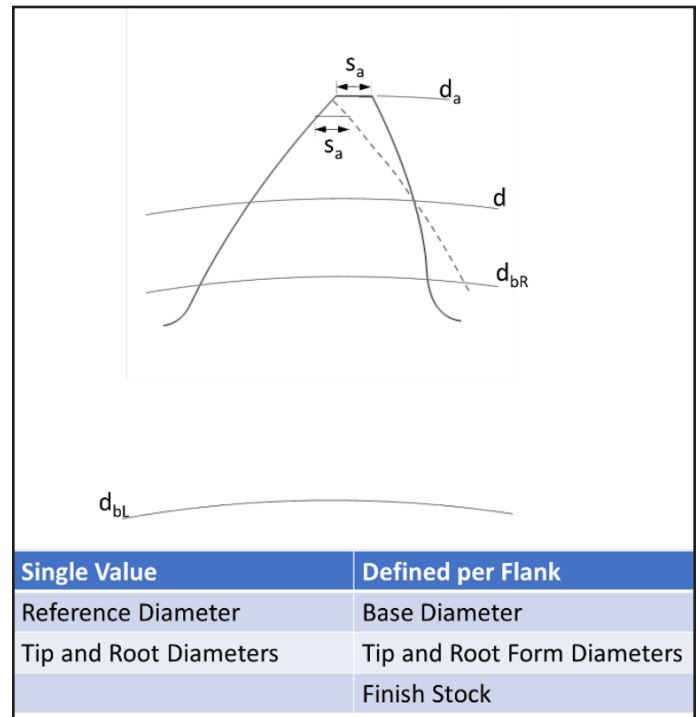


Figure 2 Asymmetric gear geometry.

Figure 1 shows the major geometry parameters for an asymmetric rack cutter, while Figure 2 shows the geometry parameters for an asymmetric gear. There are single normal module, helix angle and tip and root diameters. However, there is asymmetry in pressure angle, root geometry and chamfer geometry.

**Rating.** The existing cylindrical gear rating standards for the major gear failure modes of, e.g. — pitting and bending in ISO 6336 (Ref. 1) — are not directly applicable to asymmetric gears. Some authors have applied the methods of these standards with modifications (Refs. 2–5). Kapelevich, for example, has developed a rating method that utilizes the existing standards and equivalent symmetric tooth gears, with conversion factors based on FE analysis. Kapelevich has reported good results for the method, although it is not entirely satisfactory from a physical perspective, as it does not directly model the actual situation. Langheinrich (Ref. 4), on the other hand, developed an approach by modifying the equations of DIN 3990/ISO 6336. Sekar and Muthuverappan (Ref. 5) adapted the form and stress correction factors of ISO 6336 Method B for spur asymmetric gears.

In this paper we present an approach to the analysis of asymmetric gears based on a high-fidelity hybrid Hertzian and FE-based specialized gear loaded tooth contact analysis; this analysis method is described in the next section.

## Loaded tooth Contact Analysis

For the assessment of asymmetric gear tooth contact conditions, including load distribution, transmission error and root and contact stresses, a hybrid Hertzian and FE based loaded tooth contact analysis method was developed based on the model presented in Langlois et. al (Ref. 6) for symmetric gears.

**Hybrid hertzian and FE-based LTCA model.** The developed model is a specialized gear-loaded tooth contact analysis model. The analysis is quasi-static, performed at  $n$  discrete time steps. At each time step, first the potential contact points on the gear teeth flanks in mesh are calculated. The assumption is made that deflections of the system are sufficiently small that the potential contact points and normals do not move from their theoretical no-load locations. Applied loads can bring those points into and out of contact. However, do not move those points locations. These potential contact points are calculated from the cylindrical gear theoretical contact lines under no misalignment and no micro geometry. In addition to these “nominal” potential contact points, a set of additional potential contact points are included at the tips of the gear teeth that are points which can potentially come into contact early, prematurely, due to deflections under load (Ref. 6).

Compatibility and force equilibrium conditions are set up between the sets of potential contact points.

$$U_{k1} + U_{k2} + \varepsilon_k - \alpha \geq 0$$

Where:

1, 2 Label the pinion and wheel, respectively

$U_{ki}$  Is the elastic deformation of gear  $i$  at point  $k$

$\varepsilon_k$  Is the initial separation at point  $k$

$\alpha$  Is the rigid body approach

$$\sum_k F_k = F$$

Where:

$F_k$  Is the normal force at strip  $k$

$F$  Is the total applied normal force due to the applied torque

The first equation enforces that there is no penetration between the contacting points. The second enforces that the sum of calculated forces is consistent with the applied torque input.

The elastic deformations  $U_{ki}$  are a function of the forces, and so these equations must be solved iteratively for  $\alpha$ , which is related to the transmission error, and  $F_k$ . For the calculation of the elastic deformations, the stiffness contributions are separated into two parts. For the bulk bending stiffness of the teeth and base rotation of the teeth on the gear body, an automatically generated FE model of the gear macro geometry is used. This model is easily adaptable from symmetric to asymmetric cylindrical gears simply by using the asymmetric gear geometry for this FE model. For the contact stiffness local to the contact points, the formalism of Weber (Ref. 7) is used.

Once the load distribution across the flanks has been calculated, the contact pressures are calculated as a post-calculation with a Hertzian cylinder on cylinder formalism with the radius of curvatures given by the roll distance of the contact points. Root stresses are post-calculated by applying the calculated load distribution back on to the FE model and reading the stresses in the root area of the FE model directly.

Due to this separation between the local contact stiffness and the bulk tooth bending and base rotation stiffness, the FE model required for the calculation can have a coarse mesh. The FE mesh is not being used to solve the Hertzian contact, as this is solved by Weber’s formalism. In contrast, to perform gear-loaded tooth contact analysis in a general FE package, a very fine mesh is required at the contact points in order to capture the local Hertzian contact deformations. As a result, the specialized gear contact model takes the order of seconds to run a load condition, while a general FE package takes orders of magnitude longer. The method therefore leads to a viable design tool where multiple loads, design parameter changes and tolerance studies can be run within the design process.

**Validation of the model.** The specialized gear LTCA method for asymmetric gears described in the previous section was validated against a surface-to-surface contact analysis model in the general finite element software ANSYS. Code was written to set up the finite element model and analysis using the ANSYS parametric design language (APDL). The node positions in the FE model were defined directly from an analytical description of the geometry, including modifications to these positions for micro geometry modifications; no CAD model was used. Figure 3 shows a schematic of the ANSYS model set-up including the applied boundary conditions. The geometry parameters for one

Table 1 Asymmetric gear pair validation example geometry		
	Pinion	Wheel
Number of Teeth	27	41
Face Width (mm)	30	28
Normal Module (mm)	3	
Helix Angle (°)	0	
Centre Distance (mm)	102	
Tip Diameter (mm)	87.09	128.935
Root Diameter (mm)	74.393	116.23
Cutter Edge Radius (mm)	0.75	0.75
	Drive	Coast
Pressure Angle (°)	38	19
Contact Ratio	1.2578	1.7233

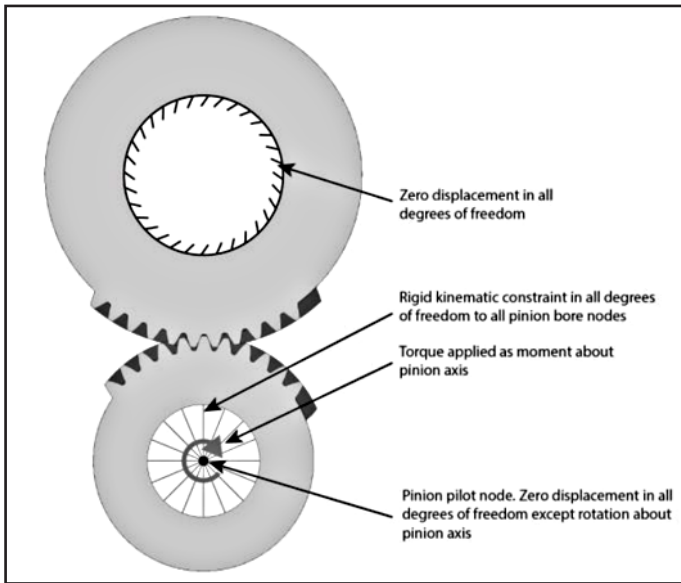


**Figure 3** Schematic diagram showing the displacement and force boundary conditions applied to the FE model.

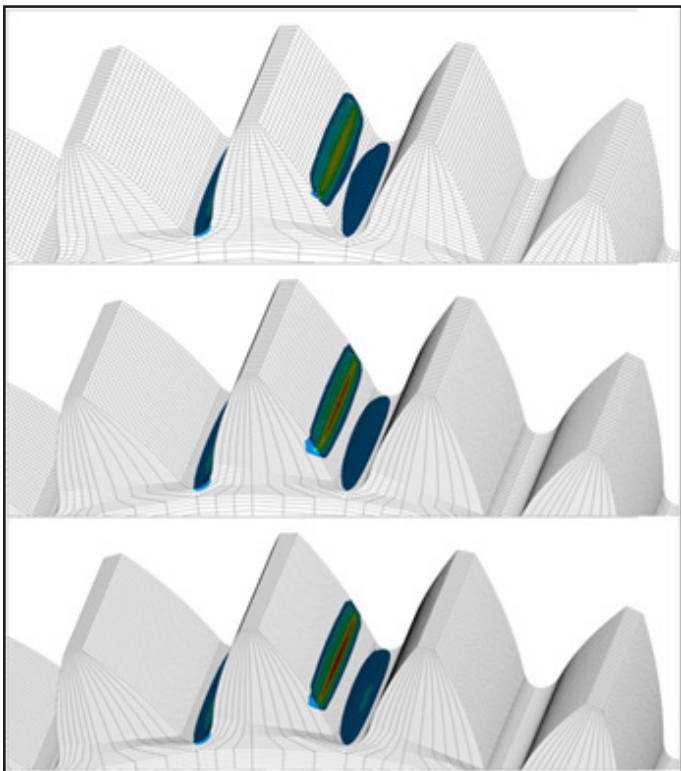


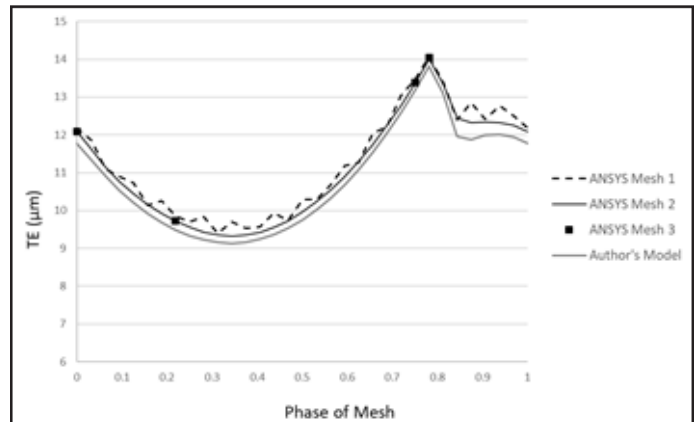
**Figure 4** ANSYS meshes; from top to bottom — mesh 1, mesh 2, mesh 3.

of the examples used for validation is given in Table 1. This particular validation example is not an automotive example. It was chosen as it has an extreme asymmetric geometry with 38 and 19 degree pressure angles on drive- and coast-flanks, respectively, and was introduced by Kapalevich (Ref.2). 15 μm of lead crowning and 13 μm of parabolic profile crowning were applied to the pinion; the gears are steel.

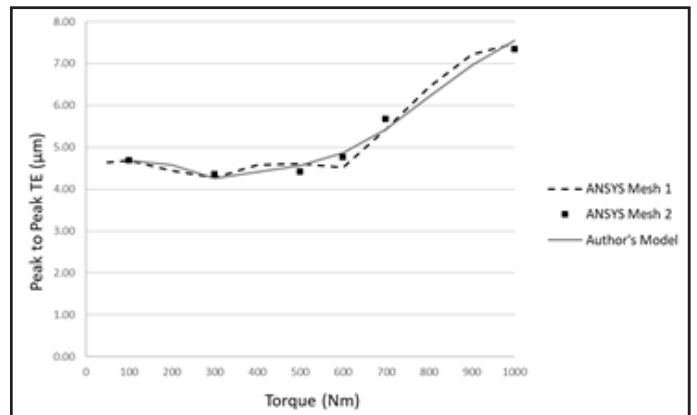
To check the accuracy of the FE model results a mesh convergence study was performed. Figure 4 shows the levels of meshes used in order to achieve convergence.

Figure 5 shows the result of one such convergence study, together with the corresponding results of the authors' model. TE is shown for the torque value for which the results were seen to be most sensitive to the FE mesh size. In this example Mesh 1 is seen to give a good prediction of mean and peak-peak TE, compared to the other meshes; however, the TE trace is not 100% smooth. Mesh 2 is seen to be smooth and gives almost identical results to Mesh 3. Similar results were seen at all loads considered — from 100 Nm–1000 Nm. A similar convergence study was performed for the results of the authors' specialized LTCA model. Excellent correlation is seen between the authors' model and ANSYS.

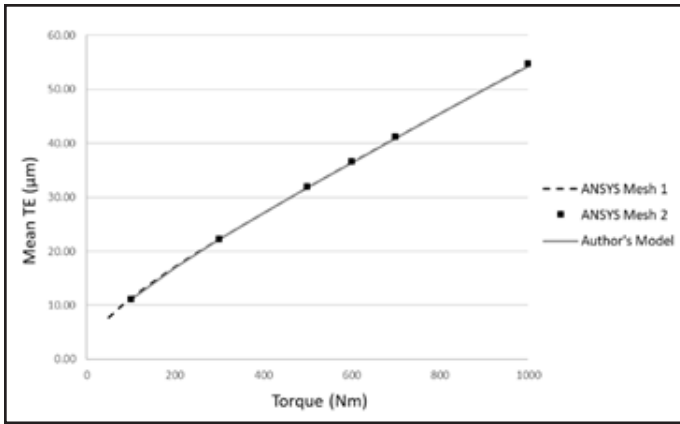
Figure 6 shows peak-peak transmission error against load, and Figure 7 shows mean transmission error against load for the authors' model and the full ANSYS analysis.



**Figure 5** ANSYS convergence study at 100Nm torque on drive flank; transmission error (μm).

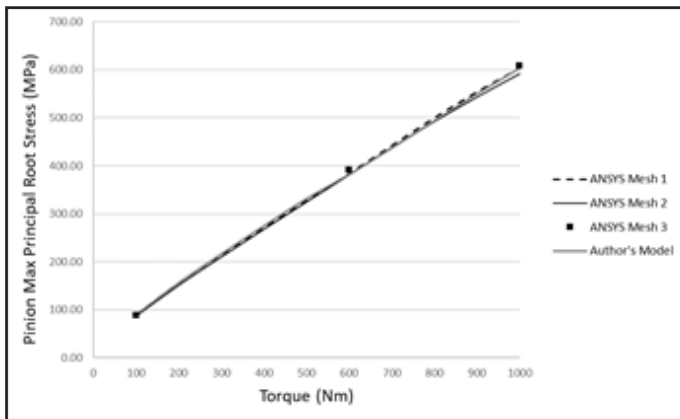


**Figure 6** Comparison of authors' model and ANSYS; peak-peak transmission error (μm) against load.



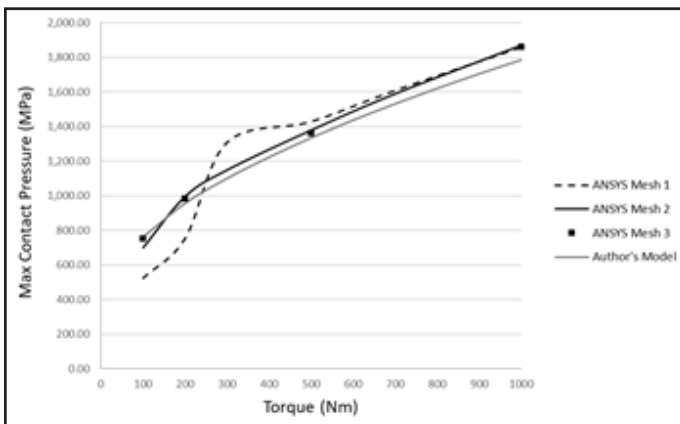
**Figure 7** Comparison of authors' model and ANSYS; mean transmission error ( $\mu\text{m}$ ) against load.

Figure 8 shows the results for the maximum principal root stress, in tension, for the pinion.



**Figure 8** Shows the results for the maximum principal root stress, in tension, for the pinion.

Finally, Figure 9 shows a comparison of the maximum contact pressure. The results for maximum contact stress are taken in the region away from any severe tip contact. It is very difficult to calculate an accurate value for the stress in edge contact regions such as extended tip contact, both via full FE or specialized gear contact analysis. In such regions the actual contact stress will be a function of the details of the actual tip shape in terms of manufacture and wear under operating. It is important to identify



**Figure 9** Comparison of authors' model and ANSYS; maximum contact stress (MPa) against load.

when such contact occurs, which such models can do, and include micro geometry such as tip and root relief in designs to avoid hard tip contact.

It is worth noting that the run times for the ANSYS model on a typical desktop with 64 GB RAM, Intel Core i7-5820K CPU were of the order of 20 minutes-per-time-step (32 time steps were run per load) for Mesh 1, 1.5 hours for Mesh 2, and 12 hours for Mesh 3. In contrast, the authors' model run times are of the order of seconds to a minute for a full load step.

## Automotive example

In this section we discuss a typical automotive application where asymmetric cylindrical gears may be considered as a design option.

Gears in typical automotive applications are mostly subjected to unidirectional loading, where the drive flank operates at greater load for longer duration compared to the coast flank. This means that the drive flank dictates the torque capacity of the gears. Asymmetric gears can be designed to increase the performance of the drive flank at the expense of the coast. This can increase the overall load capacity of the gears. Due to this reason there has been increased interest in the use of asymmetric gears within the automotive industry.

The geometry parameters used in this study are given in Table 2 and shown (Fig. 10). The original, symmetric design is based on real automotive application; the asymmetric design is an optimized asymmetric alternative to the original gear set. The

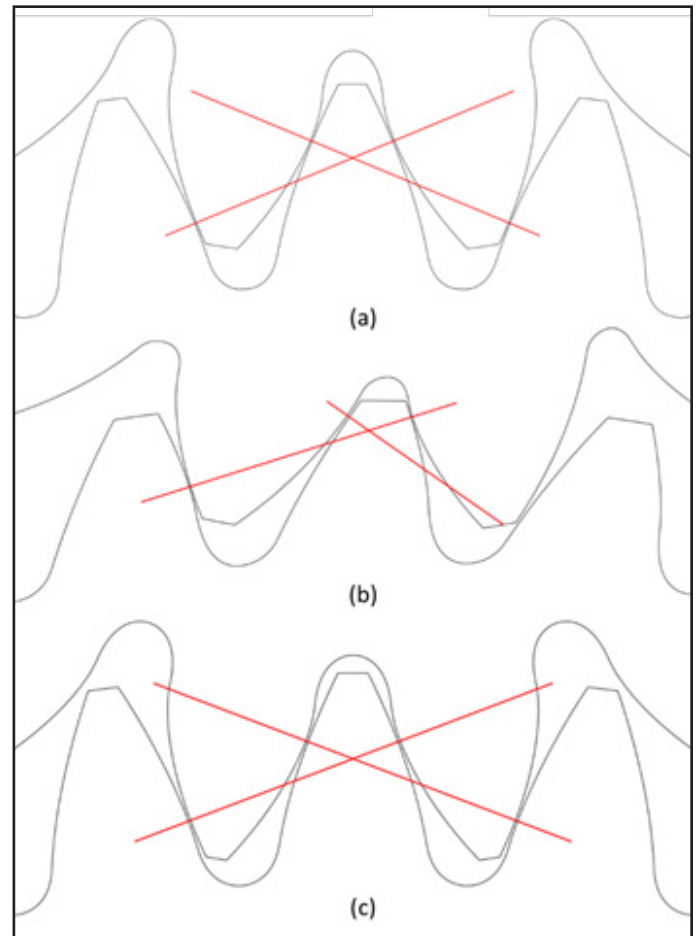


**Figure 10** Comparison of tooth shapes (a) original, (b) asymmetric and (c) HCR.

	Original		Asymmetric		HCR	
	Pinion	Wheel	Pinion	Wheel	Pinion	Wheel
<b>Gear Ratio</b>	2.45		2.53		2.45	
<b>Effective Face Width (mm)</b>			17.5			
<b>Normal Module (mm)</b>	2.2		2.5		2.21	
<b>Helix Angle (°)</b>	23		28		23	
<b>Centre Distance (mm)</b>			83			
<b>Axial Contact Ratio</b>	0.99		1.0628		1.003	
	Drive	Coast	Drive	Coast	Drive	Coast
<b>Pressure Angle (°)</b>	20		32 16		19	
<b>Transverse Contact Ratio</b>	1.7614		1.08 1.42		1.9943	

high contact ratio design (HCR) is the authors' symmetric gear optimization of the original gear set.

Even though it is possible to design asymmetric gears with high contact ratio, the option to do so was limited by the constraints for the example investigated here. One constraint was that both flanks have the same tip form diameter. This interacts with the constraint of maintaining sufficient start of active profile (SAP) to form diameter clearance. Sufficient tip thickness was also maintained for all designs.

These designs were evaluated for peak-to-peak transmission error, contact stress and root stresses using the LTCA methodology described and validated earlier in this paper.

Figure 11 shows calculated peak-to-peak transmission error for the designs detailed in Table 2. The asymmetric gear has substantially reduced transverse contact ratio, and this has an adverse impact on the transmission error. As can be seen, peak-to-peak transmission error was significantly higher on the drive flank. In the coast flank, the asymmetric gear was found to provide a lower peak-to-peak transmission error compared to the original. The best-performing design on the drive flank was the HCR, although it might be possible to achieve improved peak-to-peak transmission error behavior for asymmetric gears in certain cases, as shown by Kapelevich (Ref. 2).

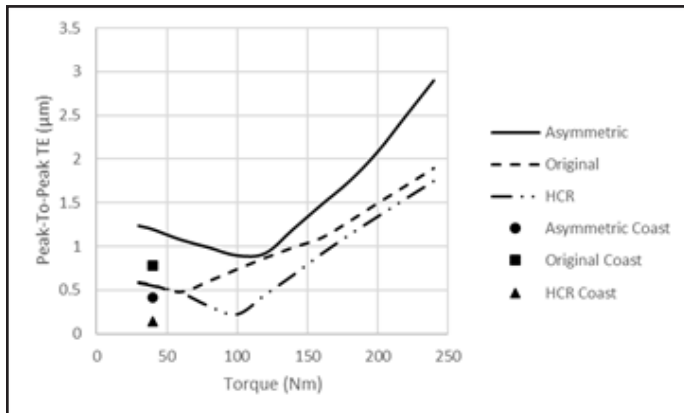


Figure 11 Comparison of peak-to-peak transmission error (µm) against load.

Figure 12 show the comparison of maximum contact stress for the three designs. For the asymmetric design, the maximum contact pressure was reduced compared to the original. This reduction is much more significant between 50 to 150Nm than at the higher loads. However, the HCR gear resulted in lower contact stresses than the asymmetric gear at all loads; it should be noted that all of these designs have some level of tip contact present.

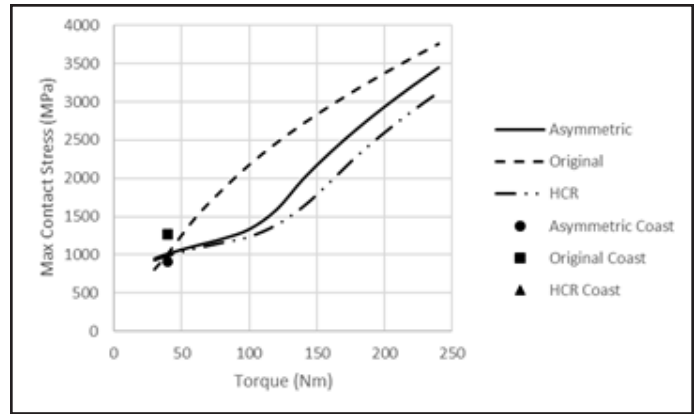


Figure 12 Comparison of maximum contact stress (MPa) against load.

Figure 13 show the comparison of maximum principal root stress, in tension, for the pinion. Using the asymmetric design, maximum tensile stress at the pinion root is reduced by approximately 10 percent in the operating range, as compared to the original design. However, it was found that the HCR gear resulted in root stresses similar to the asymmetric gear.

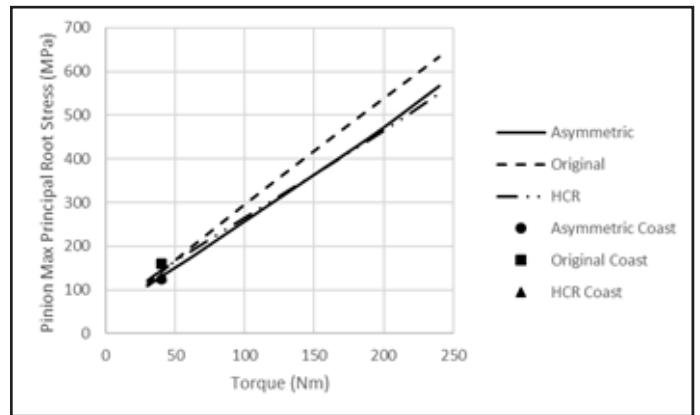


Figure 13 Comparison of pinion max principal root stress (MPa) against load.

Figure 14 shows the comparison of maximum principal root stress, in tension, for the wheel. The wheel root stresses did not improve for the asymmetric design, as compared to the original, whereas they could be improved using a HCR design.

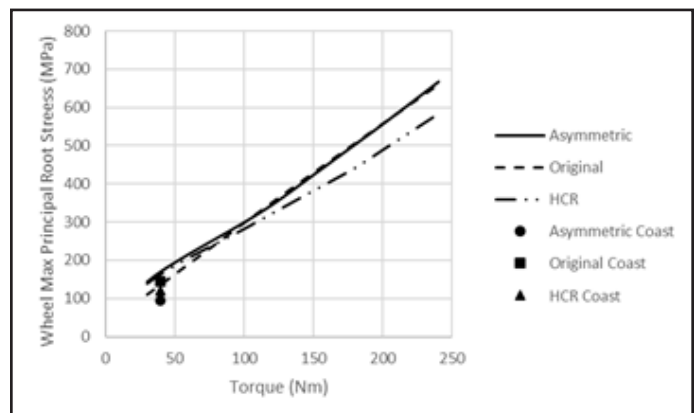


Figure 14 Comparison of wheel max principal root stress (MPa) against load.

Asymmetric gear design optimization for the given example was not very successful, although it reduced pinion root stress and contact stresses when compared to the original design. For the given constraints, it was possible to design a symmetric gear with HCR that was better than the asymmetric gear in every aspect. This indicates that although there are stated potential improvements that can be achieved with asymmetric designs, improvements are not guaranteed. A tool such as that developed by the authors is required to enable engineers to accurately and efficiently compare the advantages and disadvantages of multiple asymmetric designs between themselves and symmetric alternatives.

The designs discussed here were compared based only on transmission error, root bending stress and contact stress. Asymmetric gears might have further advantage if efficiency, scuffing and micropitting are considered. This could result due to improved radius of curvature and specific sliding due to higher pressure angle. In design settings where such criteria are important, further analysis is required. However, the efficiency effects must be investigated at the system level, as increasing the pressure angle increases the bearing loading. In addition, it is important to understand the cost repercussions of manufacturing and quality control of asymmetric gears, compared to symmetric variants.

## Conclusion

Asymmetric gears have been shown in the literature to offer significant operating advantages over symmetric gears in many applications. Increased interest is being seen in the application of asymmetric gears in the automotive industry. An efficient, validated, loaded tooth contact analysis method has been presented for the assessment of symmetric and asymmetric gear load distribution, transmission error, contact and root stresses. An automotive example was presented showing that potential benefits of asymmetric gears are not necessarily achieved when compared to optimized symmetric gear designs. This highlights the benefits of a tool such as the one presented in enabling the engineer to accurately and efficiently assess multiple gear design options — both symmetric and asymmetric. 

## For more information.

Questions or comments regarding this paper?  
Contact Paul Langlois at [Paul.Langlois@smartmt.com](mailto:Paul.Langlois@smartmt.com).

## References

1. ISO 6336, Parts 1, 2, 3. Calculation of load capacity of spur and helical gears, (2019).
2. Alex Kapelevich. *Asymmetric Gearing*, 1<sup>st</sup> Edition, CRC Press, (2018).
3. Alex Kapelevich, Yuriy Shekhtman. "Rating Asymmetric Tooth Gears," *Power Transmission Engineering*, p.40–45 (2016).
4. Langheinrich, A. "Geometrie, Beanspruchung und Verformung Asymmetrischer Stirnradverzahnungen, PhD Thesis," Technical University of Munich, (2014).
5. Muthuveerappan, P.S. "Estimation of Tooth Form Factor for Normal Contact Ratio Asymmetric Spur Gear Tooth," *Mechanism and Machine Theory* 90, p. 187–218 (2015).
6. Langlois, P., A. Baydu and O. Harris. "Hybrid Hertzian and FE Based Helical Gear Loaded Tooth Contact Analysis and Comparison with FE," *Gear Technology*, 6, p. 54–57 (2016).
7. Weber, C. "The Deformation of Loaded Gears and the Effect of their Load Carrying Capacity," Sponsored Research (Germany), British Dept. of Scientific and Industrial Research, Report No. 3, (1949).

**Dr. Paul Langlois** is the Software Engineering Director at SMT. Having worked for SMT for more than 14 years, he has extensive knowledge of transmission analysis methods and their software implementation. He manages the development of SMT's software products and is a main contributor to many aspects of the technical software development. As a member of the BSI MCE/005 committee, Langlois contributes to ISO standards development for cylindrical and bevel gears.



**Baydu AI** is a senior software engineer — gear specialist at SMT and has been working for SMT for more than 6 years. Since joining SMT, he has been contributing to development of MASTA mainly focusing on the detailed analysis of gears. Also as a member of three BSI MCE/005 committees he is participating in different working groups of the ISO TC60 committees as a UK delegate.



For Related Articles Search

asymmetric gears 

at [www.geartechnology.com](http://www.geartechnology.com)